

Ecography

ECOG-01028

de la Vega, G. J., Medone, P., Ceccarelli, S., Rabinovich, J. and Schilman, P. E. 2015. Geographical distribution, climatic variability and thermo-tolerance of Chagas disease vectors. – Ecography doi: 10.1111/ecog.01028

Supplementary material

1	Contents	
2	<i>Appendix 1: Materials and methods for open flow respirometry: CTmax and ULT....</i>	2
3	<i>Appendix 2: Supporting results: Minimum and maximum temperature. Fig. A1.....</i>	5
4	<i>Appendix 3: Figure A2. Performance for each bioclimatic variable.....</i>	6
5	<i>Appendix 4: Figure A3. Most limiting factor maps.....</i>	7
6	<i>Appendix 5: Appendix references.....</i>	8
7		

8 ***Appendix 1. Materials and methods for open flow respirometry: CTmax and ULT***

9 To measure real time CO₂ production and motor activity in unrestrained triatomines, we
10 used the high-resolution TR-2 Sable System International (SSI; Las Vegas, Nevada,
11 USA) flow-through respirometry system with a Li-Cor (LI-6251) CO₂ infrared analyzer
12 (resolution 0.1 ppm CO₂) attached to a AD-2 Activity Detector (SSI) (Lighton and
13 Turner 2004). Briefly, air free of CO₂ and H₂O was drawn at a flow rate of *ca.* 100 ml
14 min⁻¹ STP by a SS4 sub sampler (SSI), which unites a pump, needle valve and a
15 linearized mass flow meter, through 3 mm diameter low-permeability Bev-A-Line
16 tubing and a RC-M precision miniature respirometer chamber (volume *ca.* 13 ml; SSI).
17 Specimen temperatures were controlled to ± 0.2°C by a SSI's Pelt-5 temperature
18 controller and SSI's PTC-1 Peltier Effect cabinet. In order to equilibrate the temperature
19 of the respirometer chamber with that inside cabinet, the air flow passed through a
20 copper coiled tube (*ca.* 6.5 meters long) placed inside the cabinet. The temperature near
21 the respirometer chamber was measured by a thermocouple attached to a SSI TC-2000
22 thermocouple meter (accuracy 0.2 and resolution 0.01°C). The analog outputs from the
23 analyzers measuring CO₂, insect's activity, temperature of the chamber and air flow rate
24 were connected to a A/D converter (SSI UI-2, 16 bits basic accuracy = 0.05%) and
25 stored in a computer by ExpeData data acquisition software (SSI). We use a similar
26 protocol from Lighton and Turner (2004). Each individual of *Rhodnius prolixus* and
27 *Triatoma infestans* was weighed to the nearest 0.1 mg on an analytical balance (*Mettler*
28 *AJ100, OH, USA*) before and after the assay. Meanwhile, baseline air (zero CO₂) was
29 pushed through the respirometry system and the recording initiated. After at least 3 min
30 of constant baseline had been recorded, the recording was paused, the triatomine was
31 placed in the respirometry chamber and the recording re-started after 6–8min.
32 Simultaneously, the temperature profile was initiated starting with 15 min at 35°C and

33 followed by a ramp at a rate of $0.25^{\circ}\text{C}\cdot\text{min}^{-1}$ for 78 min. The final temperature was
34 maintained for 10 min and finally the program reset the cabinet temperature to 35°C .
35 CO_2 concentration in ppm, activity (arbitrary units, recorded as volts), and temperature
36 of the air within the temperature controlled cabinet, were recorded at 1 Hz until the
37 recording was manually terminated. CTmax was defined dually in terms of the species'
38 motor activity and respiratory breakdown, the activity CTmax (cessation of controlled
39 motor activity by high temperatures, e.g. start of muscle spasms (Lighton and Turner
40 2004; Chown and Nicolson 2004; Klok et al. 2004) and respiratory CTmax (cessation of
41 cyclic gas exchange). The absolute difference sum (ADS) of CO_2 production is a
42 measure of total dynamic variability, in fact, it is the cumulative sum of the absolute
43 difference between all of adjacent data points (Lighton and Turner 2004).

44 The ADS was originally used as a means of translating bi-directional position
45 measurements into an accumulated displacement vector (Lighton et al. 1993), but it has
46 proved to be of broader utility as a measure of the short-term dynamic variability of
47 data. To determine the respiratory CTmax more accurately, the inflection point of the
48 ADS residual values from 5 s before to 5 s after the suggested activity CTmax was
49 determined. This inflection point helps to determine the objective point of the
50 respiratory CTmax (Lighton and Turner 2004). After CTmax occurs, the ULT is
51 selected on the same recording, when the CO_2 trace start to be a plain line without any
52 small variations or perturbation indicating a complete cease of activity from the
53 spiracles (see about starting point of phase 5 from Figure 2).

54

55 *Data analyses*

56 The following corrections and conversions were made from the CTmax data recordings:
57 (1) CO_2 baselines were subtracted assuming a linear drift; (2) CO_2 in ppm was

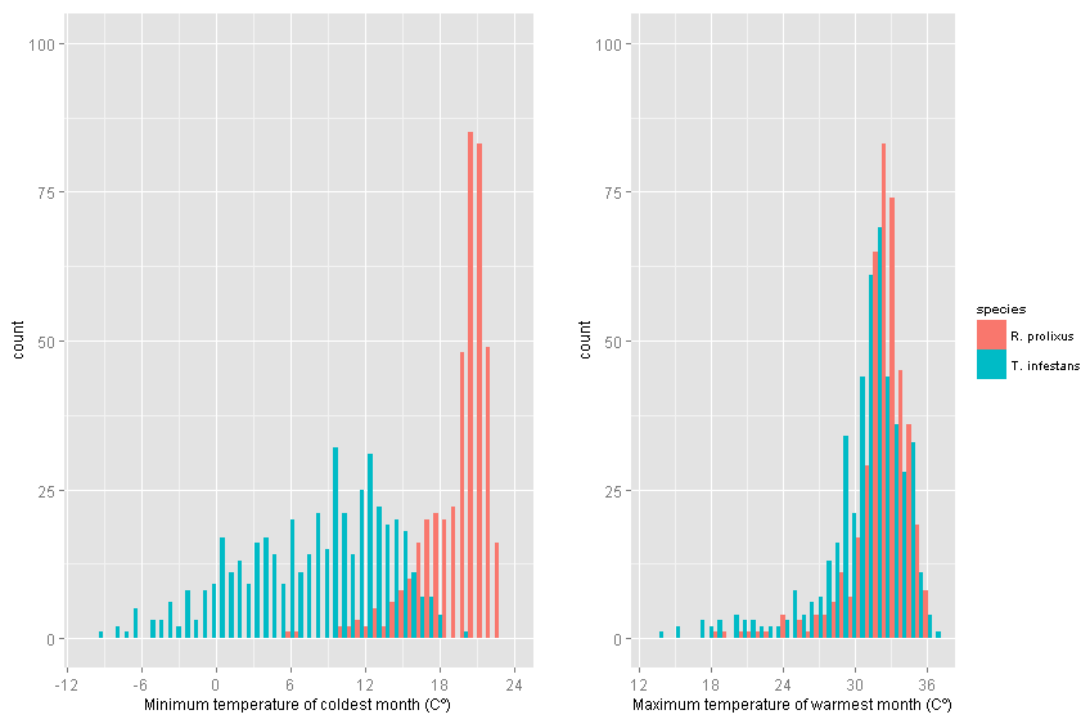
58 converted to $\mu\text{L h}^{-1}$ (for formulae see: Lighton 2008) and (3) activity and CO_2
59 productions were converted to ADS and data stored into two new different channels.
60 After corrections and conversions were made, the seven distinct phases described by
61 Lighton and Turner (2004) were measured and analyzed from the CO_2 trace of the
62 recording: (1) the equilibration phase during which VCO_2 was constant, (2) ramping
63 began, and the VCO_2 increased exponentially; (3) a ‘premortal plateau’ phase, during
64 which VCO_2 did not increase with temperature; (4) a ‘mortal fall’ where both spiracular
65 control and activity abruptly ceased; (5) a ‘postmortal valley’, a low point in post-
66 mortal VCO_2 ; (6) the ‘postmortal peak’ (VCO_2 rose again); and (7) a classic exponential
67 decay.

68 Prior to analysis, data were inspected for normality and equality of variances using
69 Shapiro–Wilk and Levene tests respectively. In most cases data were normally
70 distributed and homoscedastic, when necessary variables were transformed to meet the
71 model’s assumptions. Post-mortal Valley VCO_2 and VCO_2 at CT_{max} data were LOG-
72 transformed. Means are accompanied by standard deviations (SD) and compared by t-
73 test; $p < 0.05$ was considered significant. The global alpha error was corrected by
74 Bonferroni correction (twelve variables of CT_{max} analysis, $p < 0.004$; and 2 variables for
75 CT_{min} analysis, $p < 0.025$). Species were also compared by ANCOVA of mass-
76 independent critical thermal limits with body mass as a covariate.

77

78 **Appendix 2. Supporting results: Minimum and maximum temperatures**

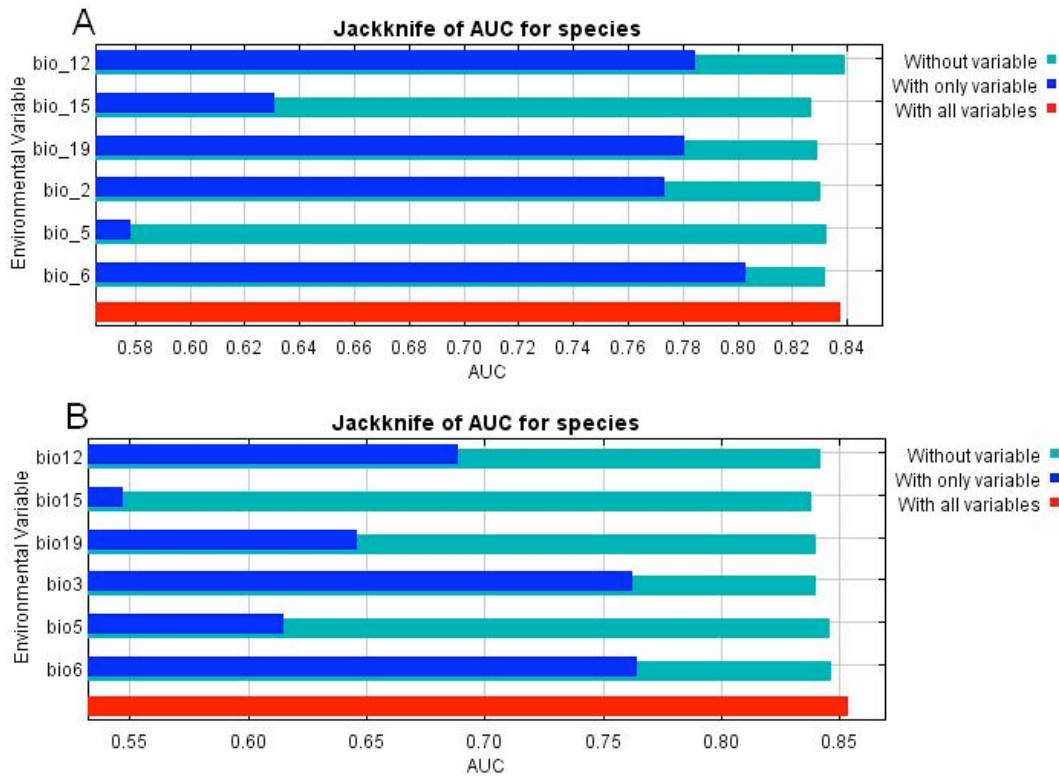
79 The distributions of the relative frequencies of minimum temperature of the coldest
80 month and the maximum temperature of the warmest month recorded over the
81 geographic distributions of *R. prolixus* and *T. infestans* are shown in **Fig A1**. *R. prolixus*
82 shows a strong dominance towards high values of both the minimum and the maximum
83 temperatures of coldest and warmest months, respectively. On the other hand, *T.*
84 *infestans* was distributed relatively equally across minimum temperature of the coldest
85 month, but with a strong dominance towards the high values of maximum temperatures
86 of the warmest month (left plot). Both species show the same pattern of distribution of
87 the maximum temperature values (right plot).



88

89 **Figure A1. Frequency of extreme temperatures.** Distributions of the relative
90 frequencies of minimum temperature of the coldest month (left) and the maximum
91 temperature of the warmest month (right) for the geographical data of *R. prolixus* and *T.*
92 *infestans*.

93



95

96 **Figure A2. Performance for each bioclimatic variable.** Jackknife test of variable
 97 importance showing how each bioclimatic variable affects Maxent prediction for *R.*
 98 *prolixus* (A) and *T. infestans* (B). Environmental variable with the highest training gain
 99 used in isolation is considered to contain the highest relative influence on the AUC of
 100 the model.

101

102

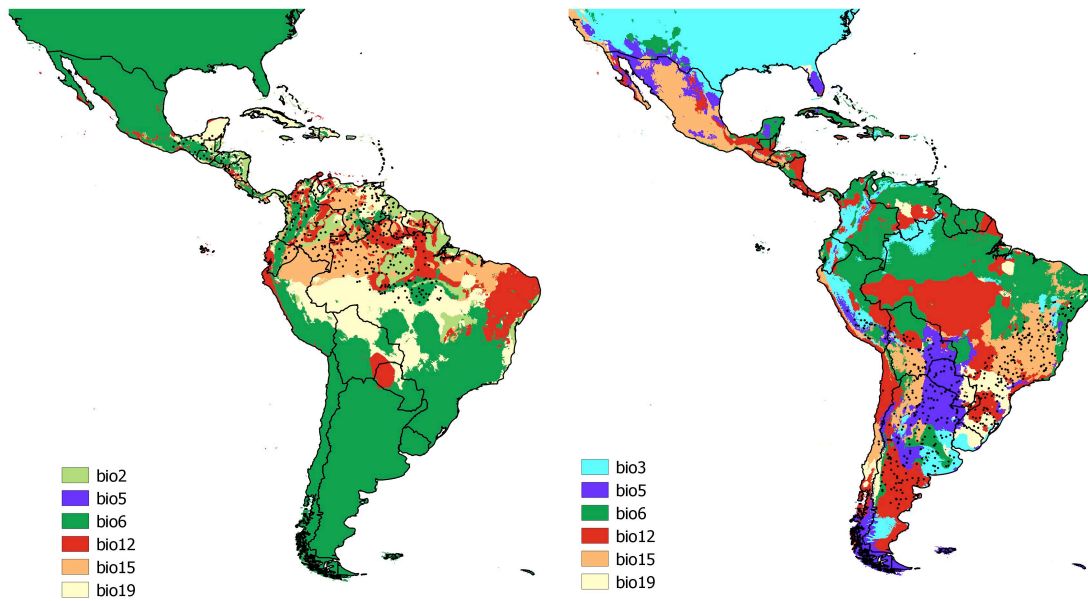
103

104

105

106

107



109

110 **Figure A3. Most limiting factor maps for models distribution. *R. prolixus* (right) and**

111 *T. infestans* (left). A limiting factor map shows the relationship between the model

112 performance and the predictors variables at each pixel (for details see Elith et al. 2010

113 and Hill et al. 2012).

114

115

116 *Appendix 5: References*

- 117 Chown, S.L. and Nicolson, S.W. 2004. Insect Physiological Ecology: Mechanisms and
118 Patterns. - Oxford Univ. Press.
- 119 Elith, J. et al. 2010. The art of modeling range-shifting species. - Methods Ecol. Evol. 1:
120 330–342.
- 121 Hill, M.P. et al. 2012. Understanding niche shifts: using current and historical data to
122 model the invasive redlegged earth mite, *Halotydeus destructor*. - Diversity
123 Distrib. 18: 191-203.
- 124 Klok, C.J et al. 2004. Upper thermal tolerance and oxygen limitation in terrestrial
125 arthropods. - J. Exp. Biol. 207: 2361-2370.
- 126 Lighton, J.R.B. 2008. Measuring Metabolic Rates: A Manual for Scientists. - Oxford
127 Univ. Press.
- 128 Lighton, J.R.B. and Turner, R.J. 2004. Thermolimit respirometry: an objective
129 assessment of critical thermal maxima in two sympatric desert harvester ants,
130 *Pogonomyrmex rugosus* and *P. californicus*. - J. Exp. Biol. 207: 1903-1913.
- 131 Lighton, J.R.B. et al. 1993. The energetics of locomotion and load carriage in the desert
132 harvester ant *Pogonomyrmex rugosus*. - J. Exp. Biol. 181: 49-61.
- 133